Analytical and Bioanalytical Chemistry
https://doi.org/10.1007/s00216-021-03564-5

PAPER IN FOREFRONT

Dual colorimetric strategy for specific DNA detection by nicking endonuclease-assisted gold nanoparticle signal amplification

Monisha Elumalai[1] · Andrey Ipatov[1] · Joana Carvalho[1] · Joana Guerreiro[1] · Marta Prado[1]

Received: 27 May 2021 / Revised: 5 July 2021 / Accepted: 19 July 2021

Abstract

The continuous spread of invasive alien species, as zebra mussel (*Dreissena polymorpha*), is a major global concern and it is urgent to stop it. Early stages of an invasion are crucial and challenging; however, detection tools based on environmental DNA analysis are promising alternatives. We present an alternative DNA target amplification strategy for signal enhancement followed by dual-mode colorimetric naked eye and optical smartphone analysis for the early detection of zebra mussel environmental DNA. Target amplification was designed based on the nicking endonuclease probe cleavage upon probe and complementary target hybridization. The cleaved/intact probe interacts with DNA-modified nanoparticles for colorimetric detection. We have demonstrated that enzyme amplification strategy enhanced 12-fold the sensitivity by naked eye detection, achieving a detection limit of ~8 nM (4.48×10^{10} copies) in controlled conditions, whereas target in complex environmental samples allowed the detection of 22.5 nM (1.26×10^{11} copies). Competitive assays also showed that the system can discriminate specific zebra mussel DNA sequences from other DNA sequences. Additionally, smartphone analysis for DNA quantification further improved the sensitivity of its detection by 130-fold, more than 2 orders of magnitude, when applied to environmental samples. The limit of detection to 0.17 nM (9.52×10^{8} copies) is based on RGB coordinates, which is especially relevant to monitor early aggregation stages, being more accurate and reducing naked eye detection subjectivity. DNA extracted from zebra mussel meat, zebra mussel contaminated river water, and non-contaminated river water samples were successfully tested. Dual-mode colorimetric detection is useful in field analysis without the need for expensive laboratory equipment.

Keywords Environmental DNA (eDNA) · Nicking endonuclease (NEase) · Gold nanoparticles · Colorimetric biosensor · Signal amplification · RGB analysis

Introduction

The fast spread of invasive alien species, such as zebra mussels (*Dreissena polymorpha*), represents one of the major threats to biodiversity and the economy. In fact, zebra mussels (*D. polymorpha*) are considered by the International Union for Conservation of Nature (IUCN) as one of the 100 most harmful invasive alien species in the world [1]. Often these species can breed quickly, dominating and unbalancing the ecosystem by competing with native species for food resources, nesting, or other environmental conditions.

Rapid spread of zebra mussels (*D. polymorpha*) is related to its reproduction cycle. The eggs are released in the water developing into free-swimming larvae which can travel long distances in water currents. The formation of larvae shells forces their settling down and attachment to hard surfaces, colonizing those regions. Several efforts are still being made to prevent zebra mussel appearance and spread. However, when these species are already settled, only management measures to prevent further its spread can be conducted [2]. Even though restraining its spread is urgent, effective methods for its early detection are still lacking [1].

Traditional methods are based on the capture and visual identification of the specimens by light microscopy and flow cytometry [3]. However, these methods are not suitable for early detection. Molecular approaches based on

Published in the topical collection featuring *Promising Early-Career (Bio)Analytical Researchers* with guest editors Antje J. Baeumner, María C. Moreno-Bondi, Sabine Szunerits, and Qiuquan Wang.

✉ Joana Guerreiro
joanarlguerreiro@gmail.com

[1] Food Quality and Safety Research Group Av. Mestre José Veiga s/n, International Iberian Nanotechnology Laboratory, Av. Mestre José Veiga s/n, 4715-330 Braga, Portugal

Published online: 10 August 2021

environmental DNA (eDNA) provide higher sensitivity than the traditional methods for invasive alien species detection, with improved capacity for the early detection [4–6].

The development of fast, easy to use/read, and low-cost tools, for decentralized analysis, is an important feature for the early detection of invasive alien species, facilitating real-time monitoring and implementation of timely corrective measures.

Alternatives based on DNA hybridization using colorimetric detection offer simple and cost-effective approaches, easy to monitor by the naked eye, and can be applied to decentralized settings [7]. Generally, visual detection mechanisms focus on immunoassays coupled with classical chromogenic systems (horseradish peroxidase [8], TMB [9]), fluorescence assays, enzyme colorimetric catalytic reactions, and metal nanoparticle colorimetric systems. Within colorimetric detection, the most explored approach uses gold nanoparticle (AuNP)–based sensors due to its great optical features, ease of surface modification, material stability, and biocompatibility [10, 11]. Colorimetric detection of DNA commonly uses two strategies, one based on nanoparticle aggregation induced by interparticle cross-linking and non-cross-linking detection based on binding properties of single- and double-stranded DNA towards unmodified nanoparticles. Despite the advantages of AuNP colorimetric assays, constraints associated with the sensitivity might hinder their applicability for early detection of invasive alien species.

Sensitivity enhancement of DNA detection has been achieved by incorporating labeling molecules (electroactive molecules, redox complexes, metal ions), integrating amplification approaches, and/or incorporation of nanomaterials [12, 13]. Within the amplification strategies, the two most common are the target- and signal-based approaches [14, 15]. Target-based approaches produce copies of a specific target continuously, in a cyclic process. The most typical example is polymerase chain reaction (PCR). PCR allows exponential growth of a specific DNA target sequence through a series of cycles of temperature changes. Several alternatives to PCR allowing an isothermal amplification of the specific target DNA, such as loop-mediated isothermal amplification (LAMP), recombinase polymerase amplification (RPA), and other techniques, are also being successfully applied [13, 16]. Signal-based amplification approaches were developed to attain ultrasensitive detection by enhancing the readable signal. Enzyme-assisted target recycling approach is one of the signal amplification approaches that hydrolyze the phosphate diester bond in the target generating enormous amplified signals by the enzymatic reaction taking place in the system in a cyclic manner within few hours or sometimes in several minutes in turn improving the sensitivity [17]. Therefore, from typical target DNA amplification approaches using PCR to isothermal amplification, or by enzyme signal-based amplification strategies, several approaches have been developed and combined with colorimetric detection [17, 18] including CRISPR/Cas systems [19].

Among these enzyme-based approaches, it is interesting to highlight nicking endonuclease-based signal amplification which diverges from the conventional restriction endonuclease on the cleaving methodology. Nicking endonucleases (NEase) cut only one strand of the double-stranded DNA at a specific recognition nucleotide sequence, leaving the other strand intact, in contrast to the traditional restriction endonucleases that cleave both strands of the duplex DNA [20]. Nicking endonuclease-assisted signal amplification, an enzyme signal-based amplification, is a simple and effective approach that can further enhance the specificity and sensitivity of the conventional colorimetric sandwich assays. The improvement of the detection limit of colorimetric assays for short DNA sequences is even more relevant when analyzing complex matrices. Additionally, nicking endonuclease-assisted signal amplification has great potential for ultrasensitive DNA detection due to its high efficiency in single-strand cleavage for multiple times [20, 21]. Still, naked eye colorimetric detection is not suitable for DNA quantification, requiring bulky and expensive equipment for reliable data analysis [22].

Smartphones or tablets are currently broadly available and offer the advantage for imaging, data analysis, and communication. A wide variety of data analyses have been explored, using photothermal imaging to monitor target-dependent temperature changes [23], colorimetric detection through RGB [24], chemiluminescent intensity [25], smartphone-based particle diffusometry platform [26], and variation and fluorescence-based detection compatible with common RGB analysis [24, 27]. These strategies efficiently eliminate the dependence on expensive instrumentations. Thus, smartphones can be used as portable and versatile monitoring devices to be used in the field [28].

Smartphone-based colorimetric detection systems use the acquired images to evaluate the sensor performance, assessed through RGB color space, enabling to accurately distinguish color differences with high sensitivity.

Herein, we report a novel highly sensitive strategy for dual-mode detection of eDNA sequences specific from zebra mussel, based on nicking endonuclease signal amplification combined with gold nanoparticles for colorimetric readout, enhancing 12-fold the sensitivity by the naked eye, whereas smartphone-based detection improved the sensitivity of DNA detection by 130-fold, more than 2 orders of magnitude in environmental samples.

The dual-mode detection through both naked eye and smartphone image analysis enables simultaneous visual

colorimetric detection and digital quantification of eDNA. Thus, the system can provide additional eDNA information even when physiological limitations and subjectivity of the human eye become an issue. The rapid and specific eDNA monitoring with higher sensitivity analysis is achieved enabling on-site detection without sophisticated laboratory instrumentation, facilitating its implementation in decentralized settings. This system is a great improvement when compared to the current methodologies available for early detection of invasive alien species.

Materials and methods

Materials and reagents

DNA sequences unmodified and thiol modified at 3′ and 5′ end were purchased from Stabvida (Caparica, Portugal). Nicking endonuclease (NEase) Nt.AlwI kit was purchased from New England Biolabs (Ipswich, MA, USA).

Tetrachloroauric acid ($HAuCl_4 \cdot 3H_2O$), sodium citrate tribasic dihydrate, disodium hydrogen phosphate, sodium chloride (NaCl), sodium hydroxide (NaOH), nitric acid (HNO_3), hydrochloric acid (HCl), sodium dodecyl sulfate (SDS), sodium dihydrogen phosphate dihydrate ($NaH_2PO_4 \cdot 2H_2O$), sodium phosphate dibasic (Na_2HPO_4), potassium cyanide (KCN), sodium citrate dihydrate, and citric acid were purchased from Sigma-Aldrich (Sigma-Aldrich, St. Louis, MO, USA).

Phosphate buffer (PB), 0.1 M, pH 7 was prepared with $NaH_2PO_4 \cdot 2H_2O$ and the Na_2HPO_4 in Milli-Q grade water (MQ) followed by pH adjustment with NaOH. Citrate buffer (CB), 80 mM, pH 3 was prepared with sodium citrate tribasic dihydrate and citric acid in MQ and adjusted with HCl. The salting buffer was composed of NaCl (2M), SDS (0.01%), and PB (10 mM). The hybridization buffer was composed of NaCl (2M) and PB (10 mM). All DNA sequences were prepared in autoclaved pyrogen, DNase, and RNase free ultrapure water. Aqua regia was prepared in the proportion 1:3 of HNO_3 to HCl.

DNA sequence selection

Gene cytochrome c oxidase subunit I (COI) and the 636-base pair (bp) fragment was selected for 50 *D. polymorpha*, as shown in Table S1 of supplementary information (SI). The identification of a short (32 bp) sequence specific from *D. polymorpha* was verified in silico using the Basic Local Alignment Search Tool (BLAST®). This software provides the statistical difference between DNA sequences available in public databases and therefore helps to identify regions providing species specificity. Iterations were also conducted to select a sequence compatible with the restriction enzyme activity by Geneious software. The selected target sequence for *D. polymorpha* with the recognition site for nicking endonuclease confers 100% specificity, as shown in SI Table S2. According to the selected target, the complementary probe and the other DNA sequences required for the detection strategy were identified using Geneious software and are listed in Table 1.

Spherical gold nanoparticle characterization and DNA loading

Spherical gold nanoparticles (AuNPs) were synthesized based on gold reduction using sodium citrate; synthesis details are described in the SI. AuNPs were characterized by UV-vis spectrophotometry, transmission electron microscopy (TEM), and dynamic light scattering (DLS) following the protocols detailed in SI. AuNPs obtained after the synthesis are defined as as-synthesized AuNPs and the as-synthesized AuNPs after centrifugation (15 min at 3000 rpm) and supernatant removal are defined as preconcentrated AuNPs while modified AuNPs are the preconcentrated AuNPs loaded with DNA strands.

The functionalization of AuNPs with DNA sequences was based on the salt-aging and pH-assisted methods. Further DNA loading quantification was also conducted, and it is described in SI.

Two sets of AuNPs were prepared by the salt-aging and pH methods and each set functionalized with different DNA sequences (DNA1 and DNA2). Further description of the used protocols is displayed in methods and materials of SI.

Optimized nicking endonuclease amplification for colorimetric detection

Briefly, the optimized reaction mixture contains 5 μL of NEB buffer (10×), 4 μL of probe (0.2 μM), 4 μL of the target with concentrations ranging from 0.2 to 0.005 μM, and 27 μL MQ for hybridization at 58 °C for 5 min to induce the formation of dsDNA. The duplexes are then nicked by adding 10 μL NEase (20 units) and incubated at 37 °C for 2 h followed by its deactivation at 80 °C for 20 min. In parallel, a control solution without target was prepared. Then, 10 μL of the previous reaction mixture was mixed with 1 μL (0.25 nM, each) of AuNPs modified with DNA1 and DNA2, 1 μL PB 0.5 mM, and 1 μL PB 0.5 mM containing 0.1 M NaCl.

The colorimetric response required optimization of several parameters such as probe ranging from 0 to 100 nM, salt (0 to 0.4 M), and NP concentrations (0.1 to 0.7 nM).

Analysis of environmental matrices and samples

Spiked samples were prepared by spiking river water non-contaminated with target DNA specific from zebra mussels

Table 1 DNA sequences selected for the detection strategy

Description	Sequence	Tm, °C*
Target (T)	5′ ATTTTAACACAAGATTTTTTGATCCAACAGGA 3′	46.6
Probe	5′ TCCTGTTGGATCAAAAAATCTTGTGTTAAAAT 3′	57.5
DNA1/AuNPs1	5′ SH-A10- ATTTTAACACAAGATT 3′	54.4
DNA2/AuNPs2	5′ TTTTGATCCAACAGGA SH-A10- 3′	43.5
Nicking endonuclease Nt.AlwI	5′ GGATCNNNN/ 3′	NA
Mismatch DNA (M)	5′ GCCCTTAGCTCTAAACGAATA 3′	41.7

**Tm*, melting temperature. [Na+] = 1 M

at different concentrations ranging from 100 to 2.5 nM, in the final solution containg the AuNP for nicking endonuclease amplification and dual-mode colorimetric detection.

Competitive assays were also conducted, to evaluate the colorimetric response in the presence of other DNA sequences (mismatch DNA). The match target and mismatch sequence (50 nM each) were tested for different concentration ratios (1, 5, and 0.2). Additional tests were also conducted by fixing the mismatch concentration at both 50 nM and 10 nM, with different target concentrations from 10 to 50 nM and from 30 to 50 nM, respectively.

Extracted and purified DNA from environmental samples were also analyzed. Extracts from zebra mussel (ZM) fresh meat, ZM stored meat (6 months, 4 °C), water contaminated with ZM meat, non-contaminated river water, and surface river water contaminated with ZM were tested.

DNA extraction and purification were carried out by using genomic DNA from food kit and purified using genomic DNA clean up kit (MACHEREY-NAGEL).

The ZM fresh meat was extra purified and preconcentrated using purification protocol (50-μL sample is purified and finally eluted in 20 μL MQ) to check the colorimetric response with high ZM DNA concentration. Prior to colorimetric DNA detection of the environmental samples, the DNA concentration of the sample was evaluated using a UV-vis spectrophotometer NanoDrop 2000c (Thermo Scientific™) and Qubit® Fluorometer using Qubit® dsDNA HS (high sensitivity) Assay Kit.

Dual colorimetric strategy based on naked eye and smartphone digital analysis

Colorimetric outcome was evaluated by visual comparison with reference colors and by the digital analysis of collected images using a smartphone iPhone 8 Plus with dual 12-MP Wide and Telephoto cameras, 1920-by-1080-pixel resolution at 401 ppi and dual-domain pixels for wide viewing angles. The distance between the smartphone camera and the sample was ~15 cm. Light conditions were controlled using the setup described in Fig. S1 of SI. Image-based colorimetric detection offers great advantages; however, data comparison might be inaccurate or introduce errors when different smartphones are used. To achieve consistent colorimetric data, several approaches to standardize the data have been proposed [29].

All standards and controls were included in a single photo for accurate color comparison. Irfan view software (www.irfanview.com) was used to determine red, green, and blue of the RGB space for each sample. These coordinates were obtained from 5 different spots for each sample within the same image and at least three images were analyzed. The coordinate average was calculated as well as R/B ratio. The data were normalized based on the control with no aggregation, designated as only NE. The correlation of DNA concentration versus R/B ratio was used as a calibration and its fitting was performed using Origin 9 (Academic) 64-bit (logistic).

Results and discussion

Colorimetric detection strategy

The signal amplification strategy is based on the hybridization between the target and complementary sequence (probe); the dsDNA form is then nicked by the nicking endonuclease. This enzyme can only cleave one of the sequences when in dsDNA form; this way the target remains intact while the probe is nicked into two smaller sequences of the same size (16 bp of ~5.4 nm). The released target is available to form another dsDNA complex, keeping this cycle until enzyme deactivation. In the absence of the target, no dsDNA is formed; thus, enzyme cutting activity remains unreactive, leaving the probe sequence intact. Colorimetric detection follows DNA amplification.

The colorimetric detection is an indirect measure of the target by identifying nicked or intact probe sequences, as shown in the scheme of Fig. 1.

When two nanoparticles come into close contact, an electromagnetic field coupling occurs inducing a localized surface plasmon resonance (LSPR) shift to longer wavelengths [30]. This effect is highly dependent on the interparticle distance and size of the formed aggregates [31].

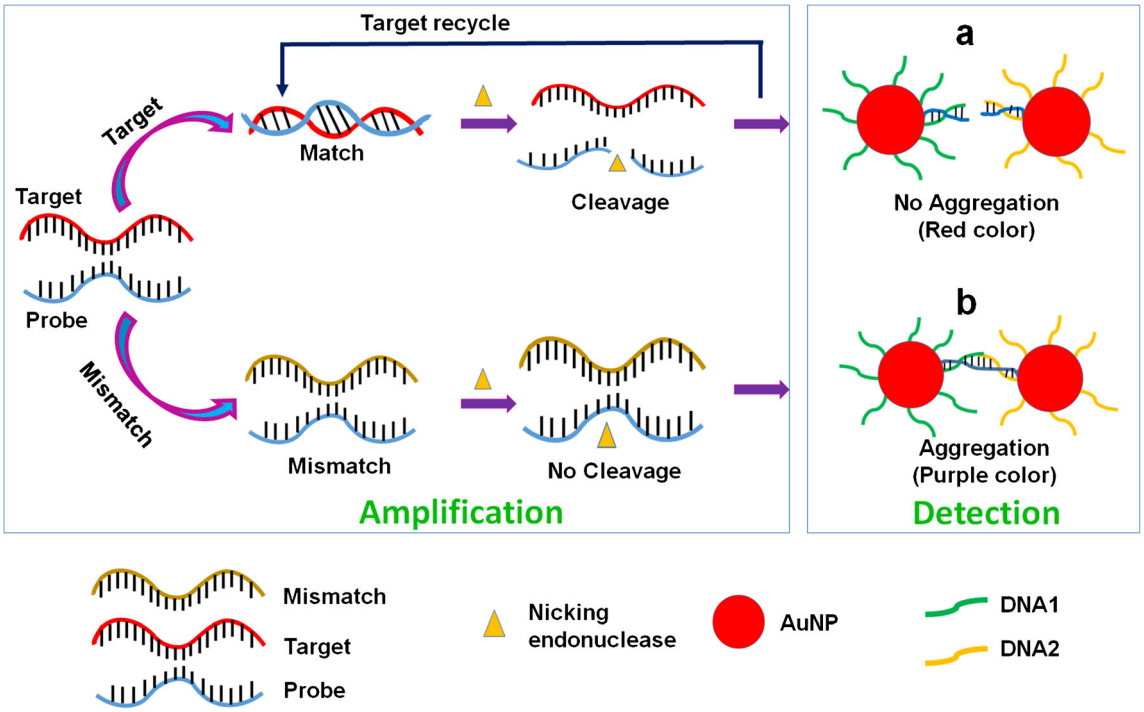

Fig. 1 Scheme of the nicking endonuclease-assisted signal-based amplification of DNA and nanoparticle-based detection

For interparticle gap between AuNPs smaller than 2.5 times the AuNP core size, the electromagnetic fields derived from the surface plasmon of the individual AuNPs may be affected by the dipolar interaction of neighboring AuNPs, resulting in significant changes in both the plasmon resonance extinction and scattering spectra [32]. Therefore, the smaller the gap, the larger the near-field coupling effect, and consequently the induced peak shift increases [33].

In this system, the colorimetric approach is based on plasmon coupling effect within gold nanoparticles (AuNPs) chemically modified with DNA sequences (DNA1 and DNA2) complementary to each end of the probe sequence. The affinity of these AuNPs depends on the length of nicked or intact probe determining the distinct colorimetric response.

In the absence of the target, the probe remains intact bringing together the two sets of DNA-AuNPs, inducing its aggregation (purple color). However, in the presence of the target, the probe sequence is nicked into two smaller sequences, each interacting with the complementary DNA-AuNPs, resulting in dispersed and stable DNA-AuNP solution (red color) [20].

Aggregation is induced by the 32-bp probe sequence, which corresponds to a gap between AuNPs of approximately 10.9 nm length. Interparticle distance of AuNPs determines the detection sensitivity of the colorimetric system; therefore, it is crucial to use AuNPs with diameters larger than the interparticle distance (AuNP size was ~23 nm) [30, 34].

Gold nanoparticle synthesis and loading

As-synthesized AuNPs (batch 2, [Au^0] of 0.11 mM) were characterized by UV-vis extinction spectra, showing a maximum peak position at 525.2 ± 0.02 nm determined through MATLAB Lorentz model fitting, as shown in Fig. 2a. Batch 1 used for DNA strand quantification was also characterized (Fig. S2 of SI). The preconcentrated AuNPs were stable and showed a maximum peak position at 526.0 ± 0.07 nm, a tiny blue shift of 0.86 nm, when compared to the as-synthesized AuNPs.

Dispersed AuNPs showed a red color (Fig. 2b) and a spherical shape with diameter size of 23.3 ± 1.6 nm (n = 200 nanoparticles) according to TEM images displayed in Fig. 2c. DLS measurements showed a hydrodynamic radius of 28.0 ± 0.82 nm for as-synthesized AuNPs while preconcentrated AuNPs showed 29.4 ± 0.47 nm. The comparison of UV-vis and DLS data for both as-synthesized and preconcentrated AuNPs indicates a negligible difference, within sample variation, and no aggregation, as can be seen in Fig. 2d. DLS data showed samples with a low polydispersity of 0.262 ± 0.01. Therefore, preconcentrated AuNPs of 141.3 nM and [Au^0] of 51.5 mM were used to proceed with DNA loading (Fig. 2).

Prior to colorimetric detection, AuNPs were loaded with thiol-polyA-modified DNA sequences (DNA1 and DNA2). The thiol end allows the chemisorption of DNA onto the gold surface while the 10 adenines' nucleotide block (polyA) work as a horizontal spacer, facilitating the upright

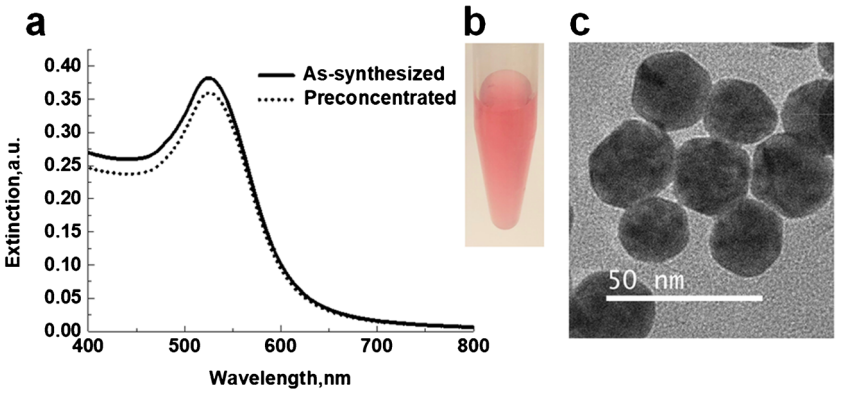

d

Samples	Hydrodynamic radius, nm	λ_{max}, nm
As-synthesized AuNPs	28.0 ± 0.82	525.17
Preconcentrated AuNPs	29.4 ± 0.47	526.03

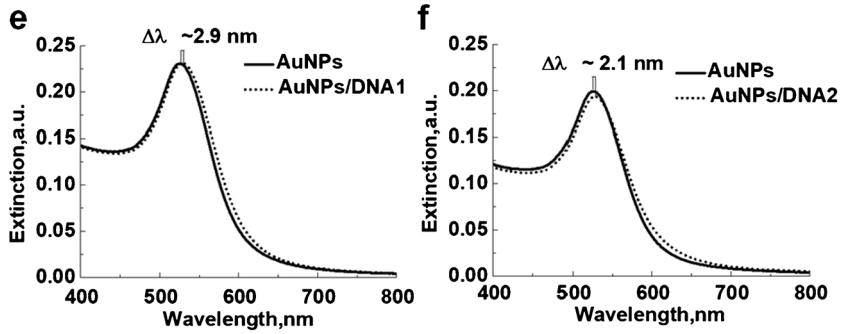

g

Samples	Hydrodynamic radius, nm	Δsize, nm	λ_{max}, nm	$\Delta\lambda_{max}$, nm
Preconcentrated AuNPs	29.4 ± 0.5	-	525.9	-
AuNPs/DNA1	40.0 ± 1.0	10.9 ± 0.7	528.9	2.9
AuNPs/DNA2	34.2 ± 0.3	5.1 ± 0.7	528.1	2.1

Fig. 2 Characterization of AuNPs. **a** UV-vis spectroscopy of as-synthesized and preconcentrated AuNPs. **b** Naked eye observation of as-synthesized AuNPs (0.11 nM [AuNPs] and 0.31 mM [Au^0]). **c** TEM image of preconcentrated AuNPs, scale 50 nm. **d** DLS data of as-synthesized and preconcentrated AuNPs at constant metallic gold concentration of 0.03 mM. **e** UV-vis spectroscopy of preconcentrated AuNPs alone and loaded with DNA by salt-aging method (0.06 mM [Au^0] and 0.16 nM [AuNPs]). **f** UV-vis spectroscopy of preconcentrated AuNPs alone and loaded with DNA by pH-assisted method (0.13 nM [AuNPs] and 0.05 mM [Au^0]). **g** DLS data of concentrated AuNPs alone and loaded with DNA1 and DNA2

conformation of the immobilized DNA and improve further hybridization [35, 36].

Probe DNA loading onto the gold surface was carried out through two different approaches, salt-aging based on high ionic strength to minimize repulsion and pH-assisted method based on DNA base protonation [37]. Therefore, the loading of DNA1 with higher guanine and thymine content was performed using salt-aging method and DNA2 by the pH method.

The DNA loading on AuNPs resulted in a red shift of the maximum LSPR band, shifting 2.9 and 2.1 nm, for DNA1 and DNA2 when compared to the preconcentrated AuNPs, as shown in Fig. 2e, f. This red shift is induced by the local refractive index change around the AuNPs due to the DNA molecules.

The presence of DNA on the gold surface was also confirmed by DLS, as shown in Fig. 2g. Hydrodynamic radius data obtained for DNA-AuNPs showed an increase in diameter of 10.9 ± 0.7 nm and 5.1 ± 0.7 nm for DNA1 and DNA2 when compared to bare AuNPs, which is within the expectable increase for these short molecules. Moreover, aggregate formation was evaluated by tracking changes on the extinction spectra at 650 nm, which was not observed during DNA loading. Estimation of the number of DNA strands per AuNPs was also determined for both sequences (data shown in Fig. S3 and Table S3 of SI).

Nicking endonuclease amplification and colorimetric optimizations

The detection of DNA from zebra mussel is based on NEase signal amplification followed by dual-mode colorimetric detection. This amplification approach in contrast with target-based amplification approaches such as PCR is based on the

DNA target capacity to keep hybridizing with the available DNA probe upon NEase activity for continuous cycles. For that, the hybridization efficiency of the target/probe and NEase cleavage efficiency were optimized. Picogreen tests were conducted to accurately quantify double-stranded DNA forms, as shown in Table S4 of SI, while Agilent Bioanalyzer assays were used to evaluate hybridization efficiency of target/probe and nicking endonuclease cleavage efficiency. Different target, probe, and NEase concentrations, as well as concentration ratios, were tested, as shown in Fig. S4, Table S5, and Table S6 of SI.

A detailed discussion of NEase system optimization is given in SI. The optimization results showed that using the same target/probe ratio at a concentration of 0.48 μM provides the best hybridization efficiency. In terms of NEase cleavage efficiency, the best results were achieved for 2-h incubation time and NEase concentration of 20 units.

The colorimetric system detects the target indirectly through full or cleaved probe (absence/presence of target), which depends on the sandwich assay between the two sets of DNA-modified AuNPs. Therefore, it is highly sensitive to probe concentration and specific of ZM target DNA. Additionally, the colorimetric system is also greatly dependent on the nanoparticle concentration; therefore, the readout was optimized for salt, probe, and AuNP concentrations.

High salt concentration minimizes electrostatic repulsion within DNA strands in solution and favors hybridization with DNA-AuNPs, contributing to faster kinetics of colorimetric response. However, above the critical salt concentration, non-specific aggregation of particles might be induced due to AuNP destabilization, resulting in the decrease of extinction peak intensity (due to the depletion of stable nanoparticles), peak broadening, and secondary peak forms at higher wavelengths.

Salt concentrations of 0.2, 0.3, and 0.4 M of NaCl prepared in PB were tested. All samples present a red color except for a 0.4 M NaCl concentration sample with a purple color, visible by the naked eye, as displayed in Fig. 3a. The purple color indicates the formation of aggregates, confirmed by the red dash line spectrum in Fig. 3b, showing a slight displacement to the right side of the LSPR peak. For easier estimation of the aggregation degree, the ratio Abs_{650}/Abs_{max} is plotted in Fig. 3c. The maximum salt concentration that avoids stability disturbance of AuNPs was 0.3 M NaCl.

The DNA-AuNP concentration also infers on the intensity of the color readout; the higher the concentration, the more intense is the red color observed. Increasing AuNP concentrations were tested ranging from 0.1 to 0.7 nM, as can be seen in Fig. 4. Sanromán-Iglesias et al. demonstrated that 4 DNA molecules per AuNPs are the minimum number of molecules to induce a meaningful color change [38]; therefore, we have also tested a much higher concentration ratio of probe and AuNPs (500 and 800) to ensure aggregate formation (using the same AuNPs). Aggregation was achieved and observed for all samples in the presence of probe when compared to the controls (absent probe). However, for high AuNP concentration (0.7 nM), the dark red color is so intense that makes visual monitoring difficult and limiting its usage (Fig. 4a).

On the contrary, for low DNA-AuNP concentrations (0.1 nM—data shown in Fig. S5 of SI), the color is faint, and even though aggregation is visible by the naked eye for higher probe concentrations, it might limit the sensitivity of the colorimetric tests for lower amounts of probe.

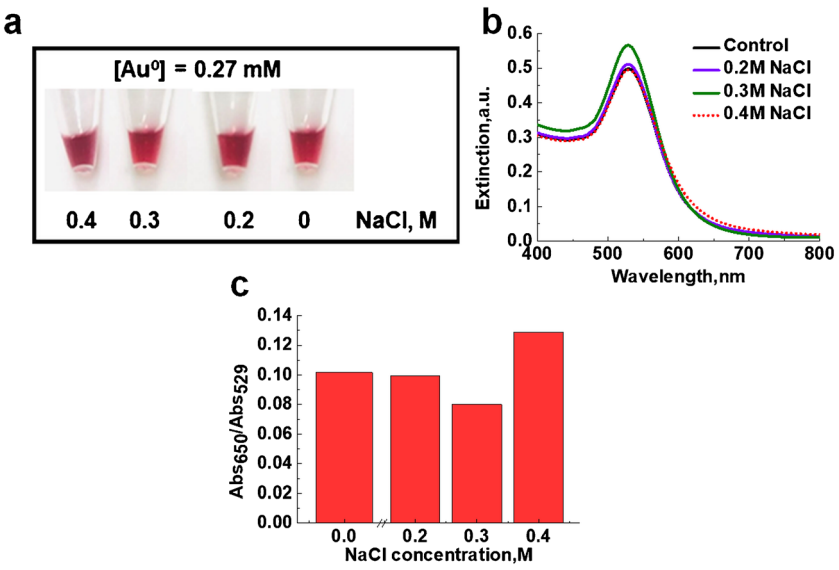

Fig. 3 Effect of different salt concentrations (NaCl) on the stability of AuNPs loaded with the two DNA sequences (~1.3 mM of metallic gold and 0.5 nM of AuNPs). (**a**) Digital image, (**b**) UV-vis spectroscopy, and (**c**) estimated degree of aggregation (Abs_{650}/Abs_{529})

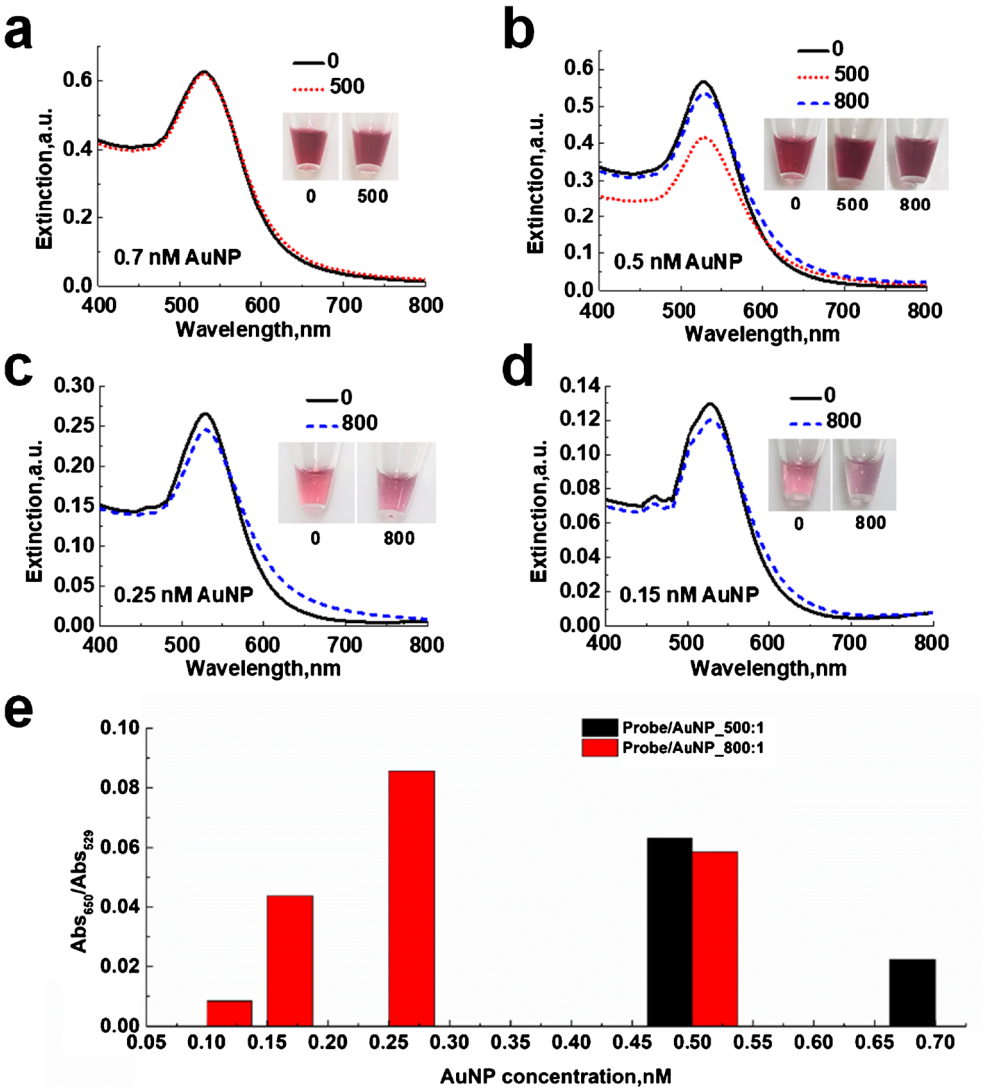

Fig. 4 Effect of AuNP concentration on the colorimetric response for (**a**) 0.7 nM, (**b**) 0.5 nM, (**c**) 0.25 nM, and (**d**) 0.15 nM and (**e**) degree of aggregation for the different AuNP concentrations and probe by AuNP ratio (500 and 800 DNA per nanoparticle). AuNPs-DNA control—no probe (black line, straight line), ratio 500 (red dotted line) and ratio 800 (blue dash lines) at 0.3 M NaCl

Specific aggregation induced by DNA can be diminished by decreasing AuNP concentration; therefore, for the concentration of 0.5 nM, a ratio of 800 (higher DNA concentration) was also tested (Fig. 4b). The degree of aggregation for both ratios showed a similar response; therefore, the following experiments with lower AuNP concentrations were only tested for the ratio of 800 (Fig. 4c, d).

The degree of aggregation, displayed in Fig. 4e, was also estimated for these data, allowing a better comparison within samples and controls (no DNA to bridge the AuNPs). The results showed 8.5-fold higher aggregation for 0.25 nM AuNP concentration when compared to 0.15 nM, for the DNA and AuNP concentration ratio of 800. For DNA and AuNP concentration ratio of 500, the increase of AuNP concentration leads to higher aggregation degrees until 0.25 nM and then follows a decreasing trend. Therefore, the concentration of 0.25 nM was the minimum AuNP concentration required to maximize colorimetric response for both ratio and the selected concentration used in further studies.

Colorimetric detection combined with nicking endonuclease-mediated signal amplification

Contrary to standard sandwich colorimetric approaches, here the target detection is achieved indirectly through detection of the probe. The presence of the target results in the duplex formation, allowing NEase to nick the probe sequence, breaking it into two shorter ssDNA sequences that interact with the two sets of DNA-AuNPs. In the absence of target, the full probe establishes a bridge with the DNA-AuNPs, bringing the NP together and inducing aggregation, whereas in the presence of the target, there is no bridging. Slight aggregation results in a decrease of both the LSPR peak and color intensity of the solution while color changes from red to purple upon large aggregate formation.

Non-specific aggregation was evaluated in NEB buffer (1×) with salt concentration 0.3 M, required for NEase-mediated signal amplification with DNA-AuNPs showing no aggregation, as displayed in Fig. S6 of SI. In these

conditions, the minimum probe concentration capable to induce aggregation was at 100 nM, for DNA-AuNPs with a concentration of 0.25 nM, which corresponds to 40 probe strands per nanoparticle (Fig. S7 of SI).

Colorimetric detection followed the amplification step and was performed using the optimized conditions of 0.3 M salt concentration, 0.25 nM of AuNP concentration, and 100 nM of probe concentration.

In parallel with the target colorimetric detection, control 1 designated as "only NEase" composed by NEase in NEB/DNAs-AuNPs (DNA1- and DNA2-modified AuNPs) with no target or probe and control 2 defined as "No NEase" composed by NEB/probe/target/DNAs-AuNPs with no nicking endonuclease were also prepared. These two controls remained stable and red. Contrary to the colorimetric response of these controls, the negative control prepared in the absence of target showed aggregation, induced by the full-length probe, within 30 min and the appearance of the purple color. All the controls worked as color references for the dual colorimetric analysis.

Different target concentrations ranging from 0 to 100 nM were also evaluated to assess the analytical colorimetric response, as shown in Fig. 5a. Three replicas (n = 3) were prepared throughout the colorimetric system evaluation. The obtained colorimetric response showed no aggregation (red color) for the target concentration range from 100 to 15 nM at a constant probe concentration of 100 nM. However, for target concentrations of 8 nM, the sample starts aggregating, showing dark purple shades, while for 2.5 nM, the color of the solution becomes less intense, and the appearance of a purple shade is observed. Thus, a limit of detection (LoD) for naked eye detection was ~8 nM (4.48×10^{10} copies).

The effect of probe concentration on the sensitivity of the system was further investigated by testing higher probe concentrations, 150 and 200 nM at a constant target concentration of 50 nM. Probe concentration of 150 nM and 100 nM behaves similarly and DNA-AuNPs remained stable, whereas the 4-fold probe concentration (200 nM) triggers non-specific aggregation, as shown in Fig. 5b. These results suggest that when probe concentration is much higher than the target (4-fold), the intact probe dominates over cleaved probes leading to aggregation, which negatively impacts the sensitivity of the system. The concentration of 100 nM increased the sensitivity of the colorimetric system.

Standard colorimetric sandwich assays use a DNA sequence to induce aggregation within AuNPs which is equivalent to our aggregation assays when only probe was present. This means that the detection limit would be in the range of 100 nM (equivalent to 5.62×10^{11} copies) (Fig. S7); however,

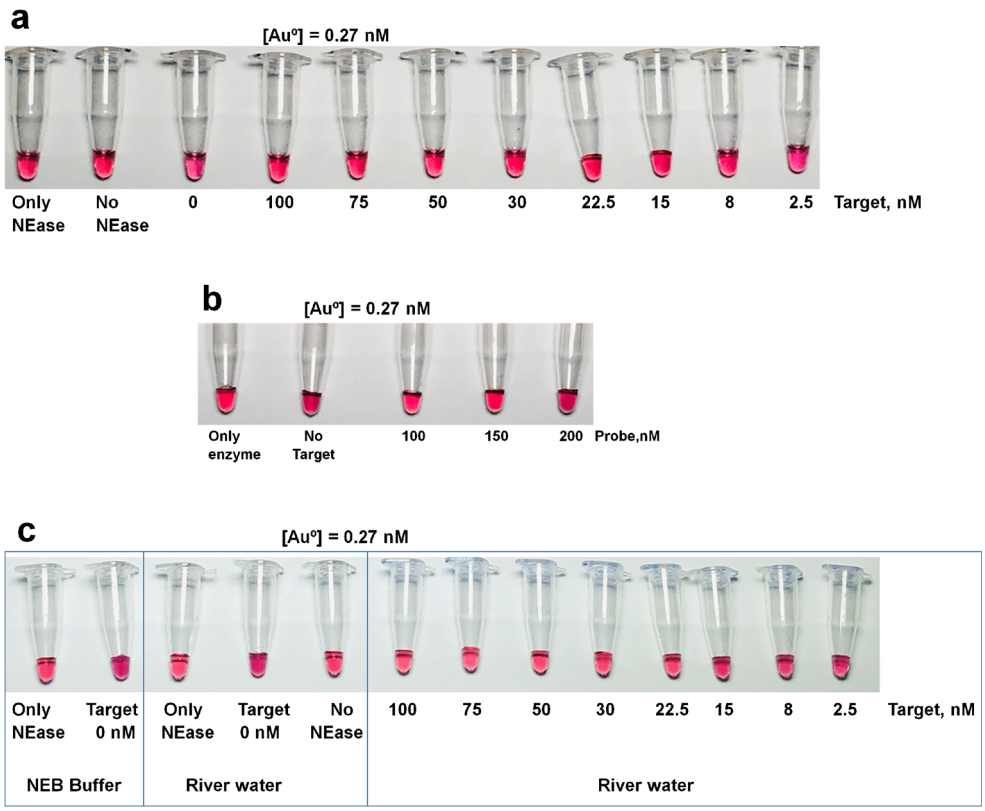

Fig. 5 Colorimetric response obtained for (**a**) different target concentrations ranging from 100 to 2.5 nM, at constant of 0.25-nM AuNP concentration ([Au^0] 0.27 mM) and probe concentration 100 nM; (**b**) effect of probe concentration at constant target concentration (50 nM); and (**c**) colorimetric response of controls (and spiked river water samples with different DNA target concentrations ranging from 100 to 2.5 nM at constant 0.25nM AuNPs ([Au^0] of 0.27 mM) and probe concentration 100 nM (n = 3)

* Control 1 "**only NEase**" - NEase in NEB/DNAs-AuNPs; Control 2 "**No NEase**" - NEB/Probe/Target/ DNAs-AuNPs

the indirect system based on NEase amplification with probe and target DNA can detect target concentrations down to 8 nM (equivalent to 4.48×10^{10} copies), showing a clear sensitivity enhancement of 10-fold.

To evaluate the sensitivity and selectivity of the colorimetric system when analyzing real samples and environmental matrices, competitive assays were carried out.

Environmental sample matrix effect and competitive assays

The effect of complex matrices on the sensitivity and selectivity of colorimetric response was evaluated by testing river water samples spiked with target DNA (fully match) and non-specific DNA sequences were tested.

River water samples were spiked with increasing target concentrations ranging from 100 to 2.5 nM, as shown in Fig. 5c, the same concentration range tested in buffer conditions. River water samples when combined with DNA-AuNPs showed no aggregation, showing no direct interference as displayed in Fig. S8 of SI, although for concentrations below 22.5 nM the system started to show purple shades, suggesting aggregation. Thus, river water samples have a slight effect on the LoD. The decrease of LoD to 22.5 nM (equivalent to 1.26×10^{11} copies) indicates that some elements present in river water samples limit by 2-fold the colorimetric response.

The calibration in river water was performed with DNA target and fully complementary probe, although to mimic environmental samples, multiple DNA sequence coexistence was evaluated. Thus, the colorimetric response in river water samples was tested in the presence of target fully complementary to the probe (match) denoted as "T" and non-complementary DNA (mismatch) denoted as "M." The mismatch sequence used is a 21-bp sequence from the same invasive species, zebra mussels, even though it is non-complementary to the probe sequence used in our colorimetric strategy. For the competitive assays, different concentrations of match and mismatch sequences were mixed during NEase amplification followed by colorimetric detection. Simultaneously, match and mismatch sequences were individually tested as a control, showing a red and purple color, respectively. Three replicas were prepared for all conditions.

Samples containing match and mismatch DNA in the concentration ratio of 1 (50:50 nM), 5 (50:10 nM), and 0.2 (10:50 nM) were tested. The colorimetric responses in the presence of a low concentration of mismatch DNA (10 nM) do not influence the colorimetric response for the concentration ratio of 5. In the opposite situation, when the concentration of match target DNA is 10 nM, lower than the detection limit, and the mismatch is 5-fold higher (50 nM), the colorimetric response remains negative for the presence of the target, as displayed in Fig. 6a.

Further analysis of match target concentrations of 30 and 40 nM in the presence of low concentration of mismatch DNA (10 nM) showed that colorimetric response remains unaffected by the presence of mismatch sequences and detection of match target is still possible, as demonstrated in Fig. 6b. In real samples, the opposite situation where mismatch sequences are in higher concentrations than the target is likely to occur. Therefore, match and mismatch sequences mixed in smaller concentration ratios (0.8, 0.6, 0.4, 0.2) were tested while keeping mismatch sequences at high concentrations (50 nM). The results are displayed in Fig. 6c.

Controls of only NEase and no target showed the expected red and purple color (aggregation), respectively. The sample with only match target (50 nM) and only mismatch (50 nM) also behaved as expected, showing a distinct red and purple color. The synergetic effect of co-interaction of match target and mismatch sequence at the tested concentrations showed that the system is capable to specifically distinguish the target DNA up to a concentration ratio (match/mismatch) of 0.4. Below this threshold ratio, for matching target concentrations of 10 nM with 50 nM mismatch target sequence (0.2 target/mismatch ratio), the system shows aggregation, not being able to detect the target DNA.

However, this ratio corresponds to a match target concentration below the sensitivity of the colorimetric system; thus, the presence of mismatch sequences does not effectively affect the colorimetric response.

In summary, the colorimetric detection demonstrated to be highly selective for the selected match target. Additionally, the system was also tested for different environmental samples. These samples included DNA extracted from *D. polymorpha* fresh and stored meat (6 months at 4 °C), DNA extracted from *D. polymorpha* tested at 90 and 58 °C (temperature during hybridization of target and probe), contaminated river water with *D. polymorpha*, and non-contaminated river water (absence of *D. polymorpha*) (data shown in Fig. S9 of SI).

An alternative hypothesis is related to the target DNA concentrations of these samples. The samples were quantified in terms of total DNA; however, the system is designed to specifically detect a target DNA sequence, present in much lower concentration when compared to the total DNA. This means that we might be near or below the naked eye detection limit, thus impossible to visualize. To test this hypothesis, an alternative quantification approach was assessed.

RGB coordinate analysis of environmental samples

The alternative to the naked eye detection of DNA is based on the analysis of RGB coordinates of digital images. RGB color coordinate analysis allowed a fast and inexpensive accurate detection of color change and further DNA target quantification.

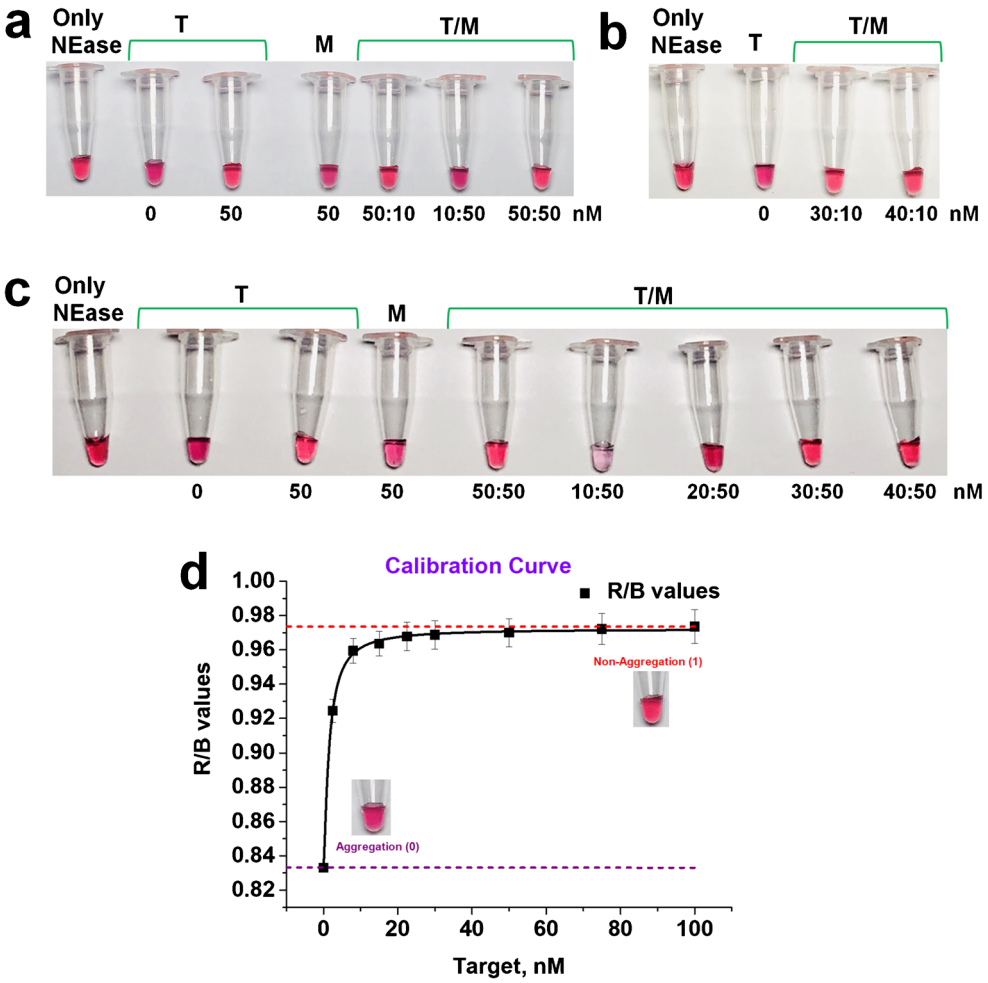

Fig. 6 Colorimetric responses of competitive assay in presence of both target and mismatch DNA (n = 3). **a** Effect of the target (T) 50 nM, mismatch (M) 50 nM, and different concentration T/M ratios in the river water. **b** Effect of different concentration ratios of T/M for low mismatch concentration of 10 nM. **c** Effect of T and M concentrations (50 nM) and decreasing concentration of T at constant 50 nM of M, in the river water. All samples with 0.25 nM AuNP concentration ([Au^0] 0.27 mM) and (**d**) calibration curve obtained by RGB data analysis (n = 3) showing R/B ratio versus target concentrations (full black line represents the sigmoidal fitting for the experimental data)

The samples induce a color change from red to purple triggered when the target is not detectable. Aggregation enhances the extinction at the blue wavelength (~ 620 nm); simultaneously the extinction peak decreases at the red wavelength (~520 nm) observed in UV-vis spectra. Therefore, to assess aggregation formation, the ratio of red and blue coordinate values (R/B) was calculated. As aggregation starts due to the decrease of target concentrations, the ratio R/B also decreases.

The target DNA concentration (x) versus ratio R/B (Y) assumes a non-linear behavior, as displayed in Fig. 6d, fitted by the sigmoidal equation of Origin software shown in Eq. 1.

$$Y = A2 + \frac{(A1-A2)}{1 + \left(\frac{x}{x0}\right)^{p}} \quad (1)$$

where the curve parameters are **A1**=0.83302, **A2**=0.97217, **x0**=1.50597, and **p** = 1.29326.

Three calibration sets were obtained, and for each, 3 digital images were analyzed to check the data consistency. Similar responses for the three replicas showed the stability of the system (n = 3). The R/B values of the digital images were normalized based on the control "only NEase" for data comparison. The normalized R/B threshold of 0.833 ± 0.002 corresponds to aggregated DNA-AuNPs as indicated by the purple dash line in Fig. 6d, meaning an absence of target, whereas well-dispersed DNA-AuNPs have the threshold of 1 (normalized based on only NEase). The red dash line in Fig. 6d corresponds to the highest target concentration (100 nM) with good dispersity. All the samples tested for the naked eye detection were also tested using RGB quantification.

The LoD using RGB coordinates was calculated based on three times the standard deviation of the blank. Our system using naked eye approach showed an LoD of ~ 8 nM (4.48×10^{10} copies) while RGB coordinates showed an LoD of ~0.17 nM (9.52×10^{8} copies). Hence, the RGB approach showed better sensitivity with a 47-fold increase in LoD in comparison with the naked eye approach.

Regarding environmental samples, digital images of the same samples analyzed previously by the naked eye that were normalized for R/B values are compared.

Similarly, calibration data by RGB analysis was based on the average of R/B values of five spots on each image and

Table 2 Estimation of DNA concentrations of environmental samples using the RGB system and total DNA concentration determined by Qubit

Environmental samples	Raw R/B values	DNA concentration, nM		DNA concentration, ng/μL	
		RGB assay	RGB assay×Df**	RGB assay×Df**	Qubit
ZM fresh meat	0.861 ± 0.008	0.59 ± 0.16	147.4 ± 39.3	1.45 ± 0.39	53
ZM stored meat	0.856 ± 0.008	0.49 ± 0.16	62.3 ± 20.4	0.61 ± 0.20	22.1*
Water contaminated with ZM meat	0.845 ± 0.009	0.15 ± 0.03	3.8 ± 0.6	0.04 ± 0.01	1.6*
River water	0.834 ± 0.001	< LoD	< LoD	< LoD	1.5*
ZM fresh meat _90 °C	0.854 ± 0.006	0.46 ± 0.13	115.2 ± 31.3	1.13 ± 0.31	53
ZM stored meat _58 °C	0.846 ± 0.001	0.28 ± 0.07	72.1 ± 17.5	0.71 ± 0.17	53

***Df*, dilution factor. *DNA concentration by NanoDrop ng/μL

three digital images of the three replicas prepared. Obtained R/B ratios were used to determine unknown concentrations of environmental samples through the curve parameters.

The determined concentration of DNA corresponds to the concentration of the selected DNA sequence instead of the total DNA concentration. In parallel, samples were also analyzed by Qubit DNA quantification, as shown in Table 2. As expected, Qubit concentrations showed much higher concentrations than RGB concentration, as it quantifies total DNA. The RGB detection is designed to quantify the concentration of the selected DNA sequence specific from ZM.

The only environmental sample with concentrations below the detection limit was the non-contaminated river water sample, which could not be quantified either by Qubit or by NanoDrop, a consistent result considering the absence of ZM DNA in this sample. Generally, all samples showed low DNA concentrations for the specific ZM sequence. Upon RGB analysis, the DNA concentration obtained for ZM stored meat showed a concentration of ~0.61 ± 0.200 ng/μL whereas ZM fresh meat showed a DNA concentration of ~1.45 ± 0.385 ng/μL. This suggests that storage for long periods (6 months) at 4 °C leads to DNA degradation and therefore less DNA available for detection.

The water contaminated with ZM showed a DNA concentration of ~0.037 ± 0.006 ng/μL indicating the presence of ZM, detectable in trace levels. The fresh ZM meat when heated at 90 °C for 5 min showed DNA concentrations of ~1.13 ± 0.307 ng/μL, whereas at 58 °C for 5 min, the concentration was 0.71 ± 0.172 ng/μL. Considering that temperature was the only variable in play, the concentration variation indicated that the formation of dsDNA at two different hybridization temperatures does not influence the detection strategy with less concentration variation. The RGB method overcomes the naked eye approach limitations, especially for samples with lower concentrations, distinguishing the different levels of aggregation when compared to visual detection. The dual-mode colorimetric approach offers an alternative to detect and identify ZM detection which can be implemented for simple and low-cost routine monitoring.

We have demonstrated that NEase-mediated signal amplification strategy enhanced 12-fold the sensitivity by naked eye detection. Moreover, the employment of smartphone digital quantification by RGB further improved the sensitivity of DNA detection by 130-fold, more than 2 orders of magnitude in environmental samples. This approach showed an LoD of 0.002 ng/μL for RGB in river water samples, which is broadly in line with other eDNA species-specific standard target amplification assays able to detect low concentrations (0.0004–0.0001 ng/μL) and isothermal amplification of eDNA field-based alternatives [39, 40, 41], confirming that RGB detection mode is a simple and good alternative for DNA quantification of invasive species.

Conclusion

We evaluated the effect of NEase-mediated signal amplification to improve sensitivity together with a colorimetric strategy for the detection of invasive alien species eDNA in environmental samples. We have demonstrated that colorimetric response using 23-nm size AuNPs combined with NEase amplification increased the detection limit 10-fold (8 nM equivalent to 4.48×10^{10} copies) when compared to standard sandwich colorimetric detection (in this work corresponds to the assays using only probe to induce aggregation, 100 nM equivalent to 5.62×10^{11} copies). Dual-mode detection of eDNA by the naked eye and/or smartphone-data image analysis enables rapid visual rapid detection and/or quantification of DNA by digital image analysis with higher sensitivity.

The effect of environmental matrices in colorimetric detection was also tested in river water samples. These matrices contribute to a slight decrease of sensitivity from 8 to 22.5 nM. Furthermore, the system was able to distinguish between target DNA (match) and non-complementary DNA sequences from the same species (mismatch) in river water samples, even when non-complementary sequence concentrations were 5-

fold higher than the target. Regarding digital RGB analysis, the presence of the specific ZM DNA sequence was confirmed and the DNA quantification of the sample was determined. Digital aided DNA quantification is especially relevant when early aggregation stages occur, and naked eye is unable to distinguish between positive and negative samples. This was observed when the different detection modes were compared.

The naked eye approach can be used for the qualitative evaluation of target DNA on samples with DNA concentrations higher than 8 nM (4.48×10^{10} copies). For concentrations below 8 nM (4.48×10^{10} copies), RGB detection mode is easier to analyze and reduces the subjectivity of the naked eye approach.

Supplementary Information The online version contains supplementary material available at https://doi.org/10.1007/s00216-021-03564-5.

Acknowledgements The authors thank the Confederación Hidrográfica del Guadalquivir (Spain) for collecting field samples.

Funding This work was supported by the Partnership Agreement with Confederación Hidrográfica del Guadalquivir (Spain) for the development of a system of early detection of the zebra mussel through analysis of environmental DNA and by the project Nanotechnology Based Functional Solutions (NORTE-01-0145-FEDER-000019), supported by Norte Portugal Regional Operational Programme (NORTE2020), under the PORTUGAL 2020 Partnership Agreement, through the European Regional Development Fund.

Declarations

Conflict of interest The authors declare no competing interests.

References

1. Clout MN, De Poorter M. International initiatives against invasive alien species. Weed Technol. 2005;19:523–7.
2. Glomski LM. Aquatic Nuisance Species Research Program: zebra mussel chemical control guide. US Army Eng Res Dev Cent ERDC/EL TR-15-9 [Internet]. 2015; Available from: http://acwc.sdp.sirsi.net/client/en_US/search/asset/1044633
3. Johansson ML, Lavigne SY, Ramcharan CW, Heath DD, MacIsaac HJ. Detecting a spreading non-indigenous species using multiple methodologies. Lake Reserv Manag [Internet] Taylor & Francis. 2020;36:432–43. Available from. https://doi.org/10.1080/10402381.2020.1797957.
4. Amberg JJ, Merkes CM, Stott W, Rees CB, Erickson RA. Environmental DNA as a tool to help inform zebra mussel, Dreissena polymorpha, management in inland lakes. Manag Biol Invasions. 2019;10:96–110.
5. Takahara T, Minamoto T, Doi H. Using environmental DNA to estimate the distribution of an invasive fish species in ponds. PLoS One 2013;8.
6. Carvalho J, Garrido-Maestu A, Azinheiro S, Fuciños P, Barros-Velázquez J, De Miguel RJ, et al. Faster monitoring of the invasive alien species (IAS) Dreissena polymorpha in river basins through isothermal amplification. Sci Rep [Internet]. Nature Publishing Group UK; 2021;11:1–11. Available from: https://doi.org/10.1038/s41598-021-89574-w
7. Dykman L, Khlebtsov N. Gold nanoparticles in biomedical applications: recent advances and perspectives. Chem Soc Rev. 2012;41:2256–82.
8. Gao Z, Lv S, Xu M, Tang D. High-index {: Hk 0} faceted platinum concave nanocubes with enhanced peroxidase-like activity for an ultrasensitive colorimetric immunoassay of the human prostate-specific antigen. Analyst Royal Society of Chemistry. 2017;142:911–7.
9. Ren R, Cai G, Yu Z, Zeng Y, Tang D. Metal-polydopamine framework: an innovative signal-generation tag for colorimetric immunoassay. Anal Chem. 2018;90:11099–105.
10. Chen H, Zhou K, Zhao G. Gold nanoparticles: from synthesis, properties to their potential application as colorimetric sensors in food safety screening. Trends Food Sci Technol [Internet] Elsevier. 2018;78:83–94. Available from. https://doi.org/10.1016/j.tifs.2018.05.027.
11. Wang G, Akiyama Y, Shiraishi S, Kanayama N, Takarada T, Maeda M. Cross-linking versus non-cross-linking aggregation of gold nanoparticles induced by DNA hybridization: a comparison of the rapidity of solution color change. Bioconjug Chem. 2017;28:270–7.
12. Yang T, Luo Z, Tian Y, Qian C, Duan Y. Design strategies of AuNPs-based nucleic acid colorimetric biosensors. TrAC - Trends Anal Chem [Internet] Elsevier Ltd. 2020;124:115795. Available from. https://doi.org/10.1016/j.trac.2019.115795.
13. Garrido-Maestu A, Azinheiro S, Fuciños P, Carvalho J, Prado M. Highly sensitive detection of gluten-containing cereals in food samples by real-time Loop-mediated isothermal AMPlification (qLAMP) and real-time polymerase chain reaction (qPCR). Food Chem [Internet] Elsevier. 2018;246:156–63. Available from. https://doi.org/10.1016/j.foodchem.2017.11.005.
14. Goggins S, Frost CG. Approaches towards molecular amplification for sensing. Analyst Royal Society of Chemistry. 2016;141:3157–218.
15. Zhao J, Chen G. Nano-inspired biosensors for protein assay with clinical applications - introduction. In: Li G, editor. Nano-inspired biosensors for protein assay with clinical applications. Elsevier; 2019. pp. xvii–xlvii. https://www.sciencedirect.com/science/article/pii/B9780128150535000167
16. Mullis K, Faloona F, Scharf S, Saiki R, Horn G, Erlich H. Specific enzymatic amplification of DNA in vitro: the polymerase chain reaction. 1986. Biotechnology. 1992;24:17–27.
17. Gerasimova YV, Kolpashchikov DM. Chem Soc Rev. Royal Society of Chemistry. 2014;43:6405–38.
18. Lobato IM, O'Sullivan CK. Recombinase polymerase amplification: basics, applications and recent advances. TrAC - Trends Anal Chem. 2018;98:19–35.
19. Li Y, Mansour H, Wang T, Poojari S, Li F. Naked-eye detection of grapevine red-blotch viral infection using a plasmonic CRISPR Cas12a assay. Anal Chem. 2019;91:11510–3.
20. Xu W, Xue X, Li T, Zeng H, Liu X. Ultrasensitive and selective colorimetric DNA detection by nicking endonuclease assisted nanoparticle amplification. Angew Chem. 2009:6981–4.
21. Zhou QY, Ma RN, Hu CL, Sun F, Jia LP, Zhang W, et al. A novel ratiometric electrochemical biosensing strategy based on T7 exonuclease-assisted homogenous target recycling coupling hairpin assembly-triggered double-signal output for the multiple amplified detection of miRNA. Analyst Royal Society of Chemistry. 2021;146:2705–11.
22. Kaarj K, Akarapipad P, Yoon JY. Simpler, faster, and sensitive Zika virus assay using smartphone detection of loop-mediated isothermal amplification on paper microfluidic chips. Sci Rep Springer US. 2018;8:1–11.

23. Cai G, Yu Z, Tong P, Tang D. Ti3C2 MXene quantum dot-encapsulated liposomes for photothermal immunoassays using a portable near-infrared imaging camera on a smartphone. Nanoscale Royal Society of Chemistry. 2019;11:15659–67.
24. Liu F, Chen R, Song W, Li L, Lei C, Nie Z. Modular combination of proteolysis-responsive transcription and spherical nucleic acids for smartphone-based colorimetric detection of protease biomarkers. Anal Chem. 2021;93:3517–25.
25. Liu D, Ju C, Han C, Shi R, Chen X, Duan D, et al. Nanozyme chemiluminescence paper test for rapid and sensitive detection of SARS-CoV-2 antigen. Biosens Bioelectron [Internet] Elsevier BV. 2021;173:112817. Available from. https://doi.org/10.1016/j.bios.2020.112817.
26. Moehling TJ, Lee DH, Henderson ME, McDonald MK, Tsang PH, Kaakeh S, et al. A smartphone-based particle diffusometry platform for sub-attomolar detection of Vibrio cholerae in environmental water. Biosens Bioelectron [Internet] Elsevier BV. 2020;167:112497. Available from. https://doi.org/10.1016/j.bios.2020.112497.
27. Severi C, Melnychuk N, Klymchenko AS. Smartphone-assisted detection of nucleic acids by light-harvesting FRET-based nanoprobe. Biosens Bioelectron [Internet] Elsevier BV. 2020;168:112515. Available from. https://doi.org/10.1016/j.bios.2020.112515.
28. Xu H, Xia A, Wang D, Zhang Y, Deng S, Lu W, et al. An ultraportable and versatile point-of-care DNA testing platform. Sci Adv. 2020;6.
29. Nixon M, Outlaw F, Leung TS. Accurate device-independent colorimetric measurements using smartphones. PLoS One [Internet]. 2020;15:1–19. Available from:. https://doi.org/10.1371/journal.pone.0230561.
30. Vial S, Nykypanchuk D, Leonard F, Prado M, Gang O. Journal of Colloid and Interface Science Plasmonic response of DNA-assembled gold nanorods : Effect of DNA linker length , temperature and linker / nanoparticles ratio. J Colloid Interface Sci Elsevier Inc. 2014;433:34–42.
31. Ghosh SK, Pal T. Interparticle coupling effect on the surface plasmon resonance of gold nanoparticles: from theory to applications. Chem Rev. 2007;107:4797–862.
32. Guo L, Jackman JA, Yang HH, Chen P, Cho NJ, Kim DH. Strategies for enhancing the sensitivity of plasmonic nanosensors. Nano Today [Internet]. Elsevier Ltd. 2015;10:213–39. Available from:. https://doi.org/10.1016/j.nantod.2015.02.007.
33. Schlather AE, Large N, Urban AS, Nordlander P, Halas NJ. Near-field mediated plexcitonic coupling and giant Rabi splitting in individual metallic dimers. Nano Lett. 2013;13:3281–6.
34. Kim IH, Kim JH, Choi JY, Shin CH, Kim JH, Bae GT, et al. Tuning the interparticle distances in self-assembled gold nanoparticle films with their plasmonic responses. Chem Phys Lett Elsevier. 2019;715:91–9.
35. Opdahl A, Petrovykh DY, Kimura-Suda H, Tarlov MJ, Whitman LJ. Independent control of grafting density and conformation of single-stranded DNA brushes. Proc Natl Acad Sci U S A. 2007;104:9–14.
36. Kimura-Suda H, Petrovykh DY, Tarlov MJ, Whitman LJ. Base-dependent competitive adsorption of single-stranded DNA on gold. J Am Chem Soc. 2003;125:9014–5.
37. Liu B, Liu J. Methods for preparing DNA-functionalized gold nanoparticles, a key reagent of bioanalytical chemistry. Anal Methods. 2017;9:2633–43.
38. Sanromán-Iglesias M, Lawrie CH, Schäfer T, Grzelczak M, Liz-Marzán LM. Sensitivity limit of nanoparticle biosensors in the discrimination of single nucleotide polymorphism. ACS Sensors. 2016;1:1110–6.
39. Blackman RC, Benucci M, Donnelly RC, Hänfling B, Harper LR. Simple, sensitive and species-specific assays for detecting quagga and zebra mussels (Dreissena rostriformis bugensis and D . polymorpha) using environmental DNA. Manag Biol Invasions. 2020;11:218–36.
40. Williams MR, Stedtfeld RD, Engle C, Salach P, Fakher U, Stedtfeld T, et al. Isothermal amplification of environmental DNA (eDNA) for direct field-based monitoring and laboratory confirmation of Dreissena sp. PLoS One. 2017:1–18.
41. Blackman RC, Ling KKS, Harper LR, Shum P, Hänfling B, Lawson-Handley L. Targeted and passive environmental DNA approaches outperform established methods for detection of quagga mussels, Dreissena rostriformis bugensis in flowing water. Ecol Evol. 2020;10:13248–59.

Monisha Elumalai is pursuing her doctoral degree in the science and technology of colloids and interfaces at the International Iberian Nanotechnology Laboratory (Portugal) in collaboration with the University of Vigo (Spain). She did her Master of Technology in the field of sensor system technology (India) and Bachelor of Engineering in the field of electronics and communication engineering (India). Her research interests focus on the development of optical biosensors, nanoparticle synthesis and characterization, DNA functionalization on nanoparticles, DNA amplification techniques, developing automated microfluidic systems, design of paper fluidic devices, developing point-of-care devices, and gas sensors.

Andrey Ipatov is Research Fellow in the food quality and safety group at International Nanotechnology Laboratory (INL). He received his PhD in natural science from Roskilde University (Denmark) with a focus on the multisensor detection of multicomponent liquids. His postdoctoral research at the Institute of the Microelectronic of Barcelona (2005–2014) was devoted to the study of ISFETs for multicomponent detection in natural and artificial liquids. He has a background in analytical chemistry, modeling, design, and fabrication of microfluidic devices and sensor integration. He is currently involved in projects which aim to develop microfluidic devices for the extraction, amplification, and detection of environmental DNA. Particularly, he designs and fabricates microfluidic cell components with a CNC milling machine, laser cutter, and other techniques. His scientific interests also include flow injection analysis, electrochemical and optical sensors, chemometrics, sensor array, development of new analytical methods, and portable systems for analysis of liquids. He is an expert on miniaturization and integration of analytical devices to produce POC devices.

Joana Carvalho is a PhD student in innovation in food safety and technology at the University of Santiago de Compostela and she has been developing her work in collaboration with the International Iberian Nanotechnology Laboratory. Her main research interests include the development and optimization of microfluidic devices for DNA-based analysis with applications to food safety, food authenticity, and environmental fields. She believes that miniaturization and automatization of well-established molecular biology techniques are the next step for more efficient analytical tools in these areas.

Joana R.L. Guerreiro received her PhD in chemistry (2015) from the University of Porto, Portugal, in straight collaboration with Aarhus University, Denmark. Afterward, she worked as Postdoctoral Researcher at iNANO (Denmark) for one year and at International Iberian Nanotechnology Laboratory (Portugal) for four years. In 2021, she was awarded with a Junior Research Position and since April she has been working at the Centre of Biological Engineering – University of Minho. Her main research interests focus on the development of optical biosensors, synthesis of metallic nanostructures, design of microfluidic systems, and paper-based devices for the detection of target analytes (biomarkers, DNA), applied to the health and environmental fields.

Marta Prado is Group Leader of the Food Quality and Safety Research Group (FQ&S) and the Foodture Cluster Coordinator at the International Iberian Nanotechnology Laboratory (INL). Her research interests are the development of new, fast, and reliable detection methodologies combining molecular biology and nano- and microfabrication for different applications for food safety and quality, working in both targeted and non-targeted methods. She has a PhD in food science and technology from the University of Santiago de Compostela (Spain) and she worked at the Joint Research Center from the European Commission (JRC-EC) in Geel (Belgium) as Scientific Officer between 2005 and 2010. In 2010, she moved to INL where she currently leads a team of 10 researchers.